Hydrocarbon/Water Interactions: Encouraging Energetics and Structures from DFT but Disconcerting Discrepancies for Hessian Indices

Kari L. Copeland[†] and Gregory S. Tschumper*,[†]

[†]Department of Chemistry and Biochemistry, University of Mississippi, University, Mississippi 38677-1848 United States

⑤ *Supporting Information*

ABSTRACT: In this work, *ab initio* electronic structure computations have been used to systematically examine the structures and energetics of nine small hydrocarbon molecules interacting with water. Full geometry optimizations and harmonic vibrational frequency calculations were performed on 30 unique dimer configurations with the MP2 method and a triple-ζ correlation consistent basis set (cc-pVTZ for H and aug-cc-pVTZ for C and O, denoted haTZ). Three different estimates of the CCSD(T) complete basis set (CBS) limit interaction energies were determined for all 30 MP2 optimized hydrocarbon/water structures, and they never deviate from their mean by more than 0.07 kcal mol^{-1}. MP2 and CCSD(T) interaction energies are virtually identical (within 0.05 kcal mol^{-1}) for dimer configurations primarily exhibiting CH···O and OH···C type interactions, but MP2 overbinds appreciably in some dimers that exhibited OH···π type interactions, by as much as 0.3 to 0.4 kcal mol^{-1} (or $\approx$10%) for the unsaturated cyclic hydrocarbons examined (1,3-cyclobutadiene, 1,3-cyclopentadiene, and benzene). Four density functional theory (DFT) methods (B3LYP, B97-D, ωB97X-D, and M06-2X) were also applied to all 30 systems with the haTZ basis set to compare optimized structures, energetics, and numbers of imaginary vibrational frequencies (n_i). The B97-D, ωB97X-D, and M06-2X functionals provide quite reasonable structures and energetics, which is consistent with other studies. This work, however, finds that all 4 DFT methods examined struggle to reliably characterize these potential energy surfaces (PESs). For example, the values of n_i from the DFT frequency calculations differed from the corresponding MP2 results for approximately one-third of the stationary points located.

1. INTRODUCTION

Weak noncovalent interactions have significant roles in many biological systems. Specifically, hydrogen bonding is one of the most important weak intermolecular forces. For example, it contributes to the crystal packing of organic molecules and to the structure of DNA and proteins.[1−4] The classical hydrogen bond is described as a hydrogen atom (H), covalently bonded to a more electronegative atom (X), interacting with an adjacent electron-rich atom or group (A), i.e. X−H···A. Often both X and A are substantially more electronegative than H (e.g., N, O, F, and Cl), and this situation is often referred to as a moderately strong hydrogen bond. Hydrogen bonds can still form, however, when X is only slightly more electronegative than H. The C−H···A weak hydrogen bond was introduced in 1937,[5] and it is now generally accepted that the C−H group is capable of donating a hydrogen bond.[6−11] It has also been shown that π electron systems can act as effective hydrogen bond acceptors, i.e. X−H···π.[12−14] Consequently, hydrocarbons can form effective hydrogen bonds,[15−28] even though not generally considered in this context.

C−H···O and O−H···π interactions between water and simple hydrocarbons have been widely studied with methane,[17,26,29−37] ethane,[38] ethene,[16,17,36] acetylene,[15,17,19,36,38−43] diacetylene,[44] cyclobutadiene,[21] and benzene.[14,25,45−62] These experimental and theoretical studies have been instrumental in demonstrating the ability of the C−H group to act as a hydrogen bond donor.

Computational studies have helped characterize the strength of these noncovalent interactions as well as their nature. For example, MP2/6−31++G(2*d*,2*p*) computations on the methane/water, ethene/water, and acetylene/water dimers revealed that the magnitude of the C−H···O interaction depended strongly on the hybridization of the C atom (sp > sp^2 > sp^3).[17] Using F$_n$H$_{3−n}$CH as a proton donor and H$_2$O, CH$_3$OH, and H$_2$CO as acceptors, Scheiner et al. reported that C−H···O and O−H···O interactions differ only in the direction of change of C−H/O−H bond lengths upon formation of hydrogen bonded complexes.[63] O−H bonds lengthen, which are accompanied by commensurate decreases in the vibrational frequency of the corresponding stretching mode (a red shift); whereas C−H bonds contract, and a commensurate increase in the vibrational frequency (a blue shift) is observed. Both interactions having the same set of forces, authors attribute this difference to a balance between electrostatic, polarization, charge transfer, and dispersion forces pushing the donor hydrogen away and exchange forces pulling the donor hydrogen closer. After analyzing MP2/6−31+G* scans of CF$_3$H···OH$_2$ and CF$_3$H···Cl− complexes, Alabugin and co-workers, alternatively, concluded that if there are weak hyperconjugation interactions, significant changes in hybridization and polarization will cause the C−H bonds involved in proton donation to contract upon formation of the complex, which are accompanied by a blue shift of the vibrational frequency.[64] Using MP2 computations on the structures of HCCH, FCCH, ClCCH, and NCH interacting with H$_2$O, Scheiner and co-workers also show that in sp hybridized alkynes, complexation causes the C−H bond to length and

vibrational frequency experience a red shift.[20] However, for sp^3 hybridized alkanes, the C−H bond contracts and a blue shift is seen, while there is little change in C−H bond distances of sp^2 hybridized alkenes.

There is also significant interest in identifying efficient density functional methods that can reliably describe these and other noncovalent interactions. Recent studies include the work of Ma and co-workers in which DFT and CCSD(T) benzene/water binding energy curves were compared.[59] Results showed that BLYP, B3LYP, PBE, and PBE0 methods underestimate the interaction, while dispersion corrected versions of the density functionals, BLYP-D, DCACP-BLYP, PBE-D, and DCACP-PBE, more closely reproduced CCSD(T) binding energy curves. Mackie and DiLabio implemented dispersion corrections by using carbon atom-centered effective potentials.[65] For the benzene/water complex, results show that the density functionals, B971, PBE, PBE1, and B3LYP, differ from CCSD(T) binding energies by 0.58, 0.60, 0.57, and 0.03 kcal mol^{-1}, respectively. For all functionals, however, deviations of the center-of-mass separation between monomers never exceed 0.1 Å. Careful calibration against benchmark databases of interaction energies and potential energy curves for a broad range of noncovalent dimers has shown that the dispersion corrected B97-D generalized gradient approximation (GGA) density functional, its locally corrected ωB97X-D hybrid variant, and the M06-2X hybrid meta-GGA functional provide a good compromise between accuracy and efficiency for a broad range of noncovalent interactions.[66−68]

This work probes the interactions of water with a variety of hydrocarbons ranging in size from methane to benzene with sophisticated quantum mechanical methods. A variety of electronic structure techniques, including some promising density functional theory (DFT) methods for noncovalent interactions, have been used to characterize the structures and energetics of CH_4 (methane), C_2H_2 (acetylene), C_2H_4 (ethene), C_2H_6 (ethane), C_4H_2 (diacetylene), C_4H_4 (cyclobutadiene), C_4H_6 (butadiene), C_5H_6 (cyclopentadiene), and C_6H_6 (benzene) interacting with H_2O (water). For each hydrocarbon/water dimer at least two stationary points were identified (one involving a C−H···O interaction and the other an O−H···π interaction). Although a variety of studies have been performed on hydrocarbon/water interactions, in the present study the CCSD(T) complete basis set (CBS) limit of the hydrocarbon/water interaction energies was determined for each structure. Two independent means were used to calculate the CCSD(T) complete basis set (CBS) limit. First, it was estimated by combining explicitly correlated MP2-R12 interaction energies with a correction for higher-order correlation effects. Second, the CCSD(T) CBS limit was determined directly with CCSD(T)-F12 single point energy computations. Results for this set of hydrocarbon/water dimers are compared to each other in order to gain insight into the nature of the hydrocarbon/water interactions at the CCSD(T) CBS limit. Furthermore, DFT results have also been compared to those from high level *ab initio* electronic structure computations to gauge their ability to reliably characterize not only the energetics of both C−H···O and O−H···π interactions between water and hydrocarbons but also the structure and nature (Hessian index) of each stationary point.

2. COMPUTATIONAL METHODS

The molecular geometry of each stationary point was optimized with second-order Møller-Plesset perturbation theory (MP2).

Harmonic vibrational frequency calculations at the same level of theory were used to characterize the nature of each stationary point as a minimum or saddlepoint on the potential energy surface (PES). For comparison, geometries were also optimized and vibrational frequencies computed with the B3LYP,[69,70] B97-D,[71] ωB97X-D,[72] and M06-2X[73] density functional theory methods. Residual Cartesian gradients were less than 1.5×10^{-5} $E_h\ a_0^{-1}$ for all optimized structures. DFT calculations used a pruned numerical integration grid, having 99 radial shells and 590 angular points per shell. A correlation consistent triple-ζ basis set that augments the heavy (i.e., non-hydrogen) atoms with diffuse functions was used for all optimizations and harmonic vibrational frequency calculations, denoted haTZ (i.e., cc-pVTZ for H and aug-cc-pVTZ for C and O).

Interaction energies (E_{int}) were computed for all optimized structures by comparing the electronic energy of the complex to those of the isolated, fully optimized fragments.

$$E_{int} = E(C_xH_y/H_2O) - E(C_xH_y) - E(H_2O) \qquad (1)$$

Electronic energies of the stationary points obtained were also computed with high level computational methods and techniques. The MP2 complete basis set (CBS) electronic interaction energy, $E_{int}^{MP2/CBS}$, for each stationary point was obtained with explicitly correlated MP2-R12 computations.[74−77] The MP2-R12 computation, which employed the A' resolution of the identity approximation, were performed with the K2−− basis set.[78] The K2−− basis set is generated from the massive K2 basis set by removing basis functions of the two highest angular momentum quantum numbers,[79,80] and they have been shown to provide nearly identical interaction energies for the benzene dimer[80] and the water dimer.[81] An additive correction for higher-order correlation effects, $\delta_{MP2}^{CCSD(T)}$, was calculated by comparing the CCSD(T)/haTZ interaction energies to those from MP2/haTZ computations

$$\delta_{MP2}^{CCSD(T)} = E_{int}^{CCSD(T)/haTZ} - E_{int}^{MP2/haTZ} \qquad (2)$$

The CCSD(T) complete basis set (CBS) electronic interaction energy, $E_{int}^{CCSD(T)/CBS}$, was estimated for all structures by combining explicitly correlated MP2-R12 interaction energies, $E_{int}^{MP2/CBS}$, with the correction term for higher-order correlation, $\delta_{MP2}^{CCSD(T)}$.[82−86]

$$E_{int}^{CCSD(T)/CBS} = E_{int}^{MP2/CBS} + \delta_{MP2}^{CCSD(T)} \qquad (3)$$

A second means was used to estimate the CCSD(T) E_{int} at the CBS limit. Explicitly correlated CCSD(T)-F12b single point energy computations were performed on each MP2 optimized structure[87] using the specialized cc-pVTZ-F12 basis set (denoted VTZ-F12)[88,89] and the corresponding default density fitting and resolution of the identity basis sets in Molpro 2009.1.[90] The perturbative triples contribution to the CCSD(T)-F12b energy was not scaled.

All optimizations and harmonic vibrational frequency computations were performed with the Gaussian 03[91] and the Gaussian 09[92] software packages. MP2-R12 computations were performed using the MPQC software package.[93,94] The Molpro 2006.1[95] program was used for CCSD(T) computations, and the Molpro 2009.1[90] program was used for CCSD(T)-F12b computations. The frozen core approximation was employed for all MP2 and CCSD(T) computations. Although explicitly correlated methods provide interaction energies close to the CBS limit, where basis set superposition error (BSSE)[96,97] vanishes,

counterpoise (CP) corrected[98,99] CCSD(T)-F12b interaction energies have also been computed to provide another means of assessing the quality of the estimated CBS limits. The standard Boys−Bernardi procedure for flexible monomers was employed as detailed in several reviews.[86,100,101]

3. RESULTS AND DISCUSSION

3.1. Structures. For each of the nine hydrocarbon/water systems (where C_xH_y = CH_4, C_2H_2, C_2H_4, C_2H_6, C_4H_2, C_4H_4, C_4H_6, C_5H_6, and C_6H_6) at least two, but as many as five, different structures have been examined. These 30 structures are shown in Figures 1, 2, 3, and 4, along with a key inter-
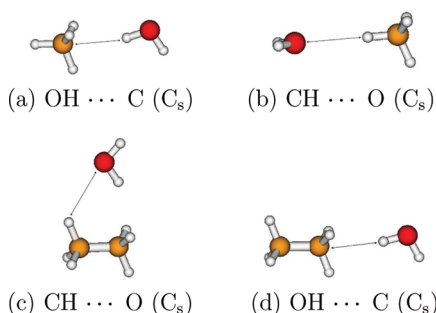
Figure 1. Configurations of water interacting with 2 simple alkene (methane and ethane).
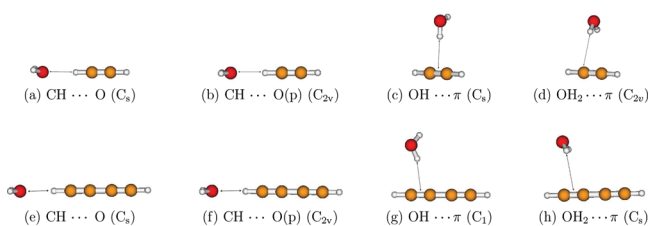
Figure 2. Configurations of water interacting with 2 linear alkynes (acetylene and diacetylene).
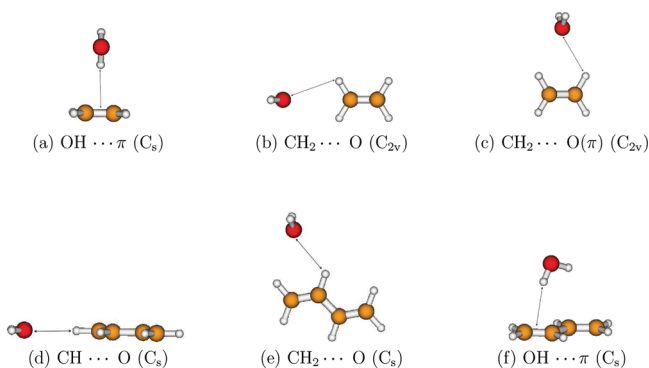
Figure 3. Configurations of water interacting with 2 acyclic alkenes (ethene and 1,3-butadiene).

molecular distance, depicted by the dashed lines. This intermolecular geometrical parameter (R) is typically the distance from the H atom participating in the hydrogen bond to either (a) the nearest C or O atom on the other fragment (denoted CH···O or OH···C) or (b) the midpoint of the C−C bond depicted in the figures (denoted OH···π or OH$_2$···π). Exceptions to these definitions include the acetylene/water OH$_2$···π structure, the benzene/water OH···π structure, and the benzene/water OH$_2$···π structure, where R denotes the distance

between an H atom in the water to the C atom shown in the corresponding figure. Note that the H atoms of the water are symmetry equivalent in the acetylene/water and benzene/water OH$_2$···π structures. The Cartesian coordinates of the MP2/haTZ optimized structures can be found in the Supporting Information.

It should be noted that alternative benzene/water OH···π and OH$_2$···π structures have been reported where the plane of the water molecule bisects carbon-carbon bonds on opposite sides of the benzene ring.[48,51,54,57,58,61] The two types of structures were found to be isoenergetic. Consequently, the present study focused on the benzene/water configurations shown in Figure 4, but a more detailed comparison can be found in the Supporting Information.

3.2. CBS Limit Interaction Energies. Estimates of the MP2 and CCSD(T) complete basis set (CBS) limits of E_{int} are reported in Table 1. Any inconsistencies in Table 1 are merely rounding errors because each entry has been computed directly from the electronic energies and rounded to two decimal places. With the exceptions of the acetylene and diacetylene structures, OH···π conformations provided more strongly bound complexes for each set of hydrocarbon/water interactions than CH···O arrangements. The OH···π configuration of the cyclopentadiene/water dimer has the largest E_{int} at the MP2 and CCSD(T) CBS limits (−4.16 and −3.79 ± 0.05 kcal mol^{-1}, respectively), while the OH$_2$···π configuration is virtually isoenergetic. These interaction energies are only about 1 kcal mol^{-1} smaller than the corresponding values for the water dimer (approximately −5 kcal mol^{-1} at both the MP2 CBS and CCSD(T) CBS limits).[102,103]

Relative to CCSD(T), MP2 tends to overbind by ≈0.3 kcal mol^{-1} (or roughly 10% of E_{int}) for OH···π type interactions with the cyclic hydrocarbons examined. The largest difference was observed for the cyclobutadiene/water dimer where the MP2/haTZ E_{int} was 0.40 kcal mol^{-1} (or 14%) larger than the corresponding CCSD(T)/haTZ value. In contrast, the correction term for higher order correlation effects, $\delta_{MP2}^{CCSD(T)}$, is very small for CH···O interactions and actually negative (indicating that MP2 slightly underestimates these types of interactions). These higher order correlation corrections are large enough to induce some qualitative changes in the energetics of hydrocarbon/water interactions. For example, the MP2 CBS E_{int} values in Table 1 indicate that the OH···π type interactions in the benzene/water dimer are slightly stronger than the CH···O interactions in the diacetylene/water dimer. At the CCSD(T) CBS limit, the situation is reversed.

It can be seen from the fourth and fifth columns of Table 1 that there is almost no difference between the two estimates of the CCSD(T) CBS limit interaction energies. In most cases, the values differed by no more than 0.02 kcal mol^{-1}. The differences only exceeded 0.1 kcal mol^{-1} for the OH···π structures of acetylene/water and diacetylene/water. Counterpoise (CP) corrected estimates of the CCSD(T) CBS limit for CCSD(T)-F12 computations are reported in the last column of Table 1. CP corrections are larger for OH···π type interactions than those for CH···O interactions. The average magnitude of the 30 CP corrections was 0.07 kcal mol^{-1} (or roughly 3% of E_{int}). The largest CP correction was 0.13 kcal mol^{-1} (or roughly 4% of E_{int}) for the OH···π structure of the benzene/water dimer. The averages of these three estimates of the CCSD(T) CBS E_{int} are reported in the first column of Table 2.

The CCSD(T) CBS E_{int} values computed here for water interacting with cyclobutadiene are very similar to those reported by
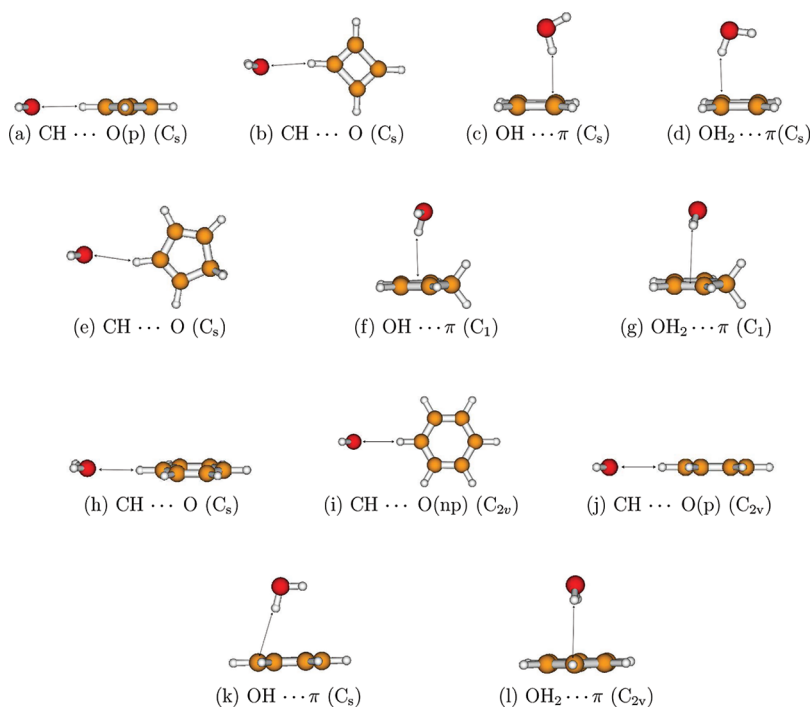
Figure 4. Configurations of water interacting with 3 unsaturated cyclic hydrocarbons (1,3-cyclobutadiene, 1,3-cyclopentadiene, and benzene).

Jing and co-workers.[21] They reported a slight preference for the OH$_2$···π over the OH···π configuration by ≈0.4 kcal mol^{-1}, which is essentially identical to our value of ≈0.5 kcal mol^{-1}. Our CCSD(T) CBS results for the unsaturated cyclic hydrocarbons examined (1,3-cyclobutadiene, 1,3-cyclopentadiene, and benzene) are also consistent with an analysis of crystal structures, where estimates of CCSD(T) CBS limit interaction energies indicated that OH···π type interactions (ranging from −3.18 to −3.24 kcal mol^{-1}) are significantly stronger than CH···O type interactions (ranging from −1.29 to −1.49 kcal mol^{-1}).[22] The interaction energies reported in Table 1 are somewhat larger because they were computed with fully optimized structures.

3.3. Comparison of Optimized Structures. The intermolecular distance, R, associated with each MP2/haTZ optimized structure is reported in Table 3, while the DFT values are reported as deviations (ΔR) from these reference geometrical parameters. The trends associated with these deviations are similar to those for the center-of-mass separations reported in the Supporting Information. Some stationary points could not be located with certain density functional methods. In these situations, the structures collapsed to another stationary point on the PES when reoptimized with a particular DFT method. This behavior was observed twice for the B3LYP, B97-D, and ωB97X-D density functionals, whereas it occurred four times for M06-2X. In the B3LYP case, the ethane/water CH···O structure collapsed to the OH···C structure and the diacetylene/water OH$_2$···π structure collapsed to the CH···O structure. With the B97-D density functional, the cyclopentadiene/water OH···π structure collapsed to the OH$_2$···π structure and the benzene/water CH···O structure collapsed to the OH$_2$···π structure reported in the Supporting Information. With the ωB97X-D density functional, the cyclopentadiene/water OH···π structure collapsed to the OH$_2$···π structure, and the CH···O benzene/water structure collapsed to the OH$_2$···π structure reported in the Supporting

Information. Finally, when optimizing with the M06-2X functional, both the OH···π and the OH$_2$···π diacetylene structures collapsed to the CH···O structure, and the cyclobutadiene/water and cyclopentadiene/water OH···π structures collapsed to their respective OH$_2$···π structure.

Some additional details regarding these optimizations are worth highlighting. Whenever a DFT optimization of an MP2/haTZ structure collapsed to a different stationary point, we also attempted to locate the stationary point by using every available DFT optimized structure as a starting point for the optimization procedure (along with the corresponding force constants from frequency calculations). If we were still not able to find the stationary point, then we also performed CP corrected geometry optimizations. Unfortunately, the CP corrected optimizations only helped us identify one stationary point with the ωB97X-D functional (the OH···π structure of the benzene/water dimer).

The minimum root-mean-square (rms) deviations between DFT and MP2 unweighted Cartesian coordinates were also determined with the superpose program in TINKER,[104] and the results are reported in Table 3. The rms deviation between B3LYP Cartesian coordinates and MP2 Cartesian coordinates differ by as much as 0.47 Å (butadiene/water OH···π structure). The B3LYP method significantly overestimates the R distance for hydrocarbon/water structures with discrepancies (ΔR) growing as large as +0.34 Å for the benzene/water OH$_2$···π structure and differing on average by 0.14 Å. The dispersion corrected B97-D and ωB97X-D functionals significantly improve results as compared to the B3LYP functional. On average, their rms deviations from the MP2 Cartesian coordinates are 0.09 Å and 0.08 Å, respectively. Similarly, the ΔR average absolute deviation decreases to 0.11 Å for B97-D and 0.06 Å for ωB97X-D. With only one deviation value larger than 0.11 Å (0.24 Å for the cyclobutadiene/water OH$_2$···π structure), the M06-2X R distances deviate by only 0.05 Å from

Table 1. CBS Limit Interaction Energies (E_{int} in kcal mol^{-1}) and Higher-Order Correlation Effects ($\delta_{MP2}^{CCSD(T)}$ in kcal mol^{-1}) for MP2 Optimized Stationary Points of Hydrocarbon/Water Dimers

structure	$E_{int}^{MP2/CBS}$ a	$\delta_{MP2}^{CCSD(T)}$ b	$E_{int}^{CCSD(T)/CBS}$ c	$E_{int}^{CCSD(T)/CBS}$ d	$E_{int}^{CCSD(T)/CBS}$ d,e
CH_4/H_2O					
OH···C	−0.96	−0.04	−0.99	−1.01	−0.97
CH···O	−0.63	−0.04	−0.66	−0.66	−0.64
C_2H_6/H_2O					
CH···O	−1.32	−0.03	−1.35	−1.37	−1.31
OH···C	−1.05	−0.05	−1.11	−1.12	−1.08
C_2H_2/H_2O					
CH···O	−2.86	−0.03	−2.89	−2.89	−2.84
CH···O(p)	−2.87	−0.02	−2.89	−2.89	−2.84
OH···π	−2.66	+0.15	−2.51	−2.62	−2.51
OH$_2$···π	−1.97	+0.04	−1.93	−1.98	−1.88
C_4H_2/H_2O					
CH···O	−3.37	−0.03	−3.40	−3.40	−3.35
CH···O(p)	−3.37	−0.03	−3.40	−3.40	−3.35
OH···π	−2.40	+0.16	−2.24	−2.35	−2.24
OH$_2$···π	−1.86	+0.05	−1.81	−1.85	−1.75
C_2H_4/H_2O					
OH···π	−2.75	+0.20	−2.54	−2.56	−2.48
CH$_2$···O	−0.83	−0.03	−0.86	−0.85	−0.82
CH$_2$···O(π)	−1.33	−0.02	−1.35	−1.33	−1.28
C_4H_6/H_2O					
CH···O	−1.13	−0.03	−1.16	−1.16	−1.13
CH···O	−1.51	−0.03	−1.53	−1.54	−1.48
OH···π	−3.22	+0.23	−2.99	−3.01	−2.91
C_4H_4/H_2O					
CH···O(p)	−1.39	−0.02	−1.41	−1.41	−1.37
CH···O	−1.51	−0.02	−1.53	−1.54	−1.49
OH···π	−3.15	+0.40	−2.75	−2.79	−2.67
OH$_2$···π	−3.63	+0.38	−3.25	−3.28	−3.16
C_5H_6/H_2O					
CH···O	−1.26	−0.04	−1.31	−1.31	−1.27
OH···π	−4.16	+0.35	−3.81	−3.84	−3.72
OH$_2$···π	−4.10	+0.30	−3.80	−3.82	−3.70
C_6H_6/H_2O					
CH···O	−1.28	−0.03	−1.30	−1.29	−1.25
CH···O(np)	−1.48	−0.02	−1.50	−1.49	−1.44
CH···O(p)	−1.28	−0.02	−1.31	−1.29	−1.25
OH···π	−3.56	+0.32	−3.24	−3.27	−3.13
OH$_2$···π	−3.46	+0.28	−3.18	−3.17	−3.06

a MP2-R12/K2−−. b $\delta_{MP2}^{CCSD(T)}$ = $E_{int}^{CCSD(T)/haTZ}$ − $E_{int}^{MP2/haTZ}$. c $E_{int}^{CCSD(T)/CBS}$ = $E_{int}^{MP2/CBS}$ + $\delta_{MP2}^{CCSD(T)}$. d CCSD(T)-F12/VTZ-F12. e Counterpoise corrected.

the MP2 values on average. Similarly, the rms deviations range from 0.01 Å to 0.20 Å, with an average of 0.05 Å.

Energetic criteria can also be used to gauge the quality of the DFT optimized structures. The data in Table 4 show how the CCSD(T) CBS limit E_{int} values change when various DFT optimized structures are used instead of the MP2 ones. The largest discrepancy between CCSD(T) CBS E_{int} determined using MP2 and DFT optimized structures is 0.41 kcal mol^{-1} for the B3LYP optimized cyclopentadiene/water OH···π structure. Nevertheless, CCSD(T) CBS interaction energies computed with B3LYP optimized structures only have an average absolute deviation of 0.10 kcal mol^{-1} from those generated with MP2 optimized structures. The differences are significantly smaller for the other three DFT methods, and CCSD(T)/CBS results obtained with the B97-D, ωB97X-D, and M06-2X structures are virtually identical to those computed with the MP2/haTZ optimized geometries. The average absolute deviations are

0.04, 0.02, and 0.02 kcal mol^{-1}, respectively, with corresponding maximum absolute deviations of 0.14, 0.06, and 0.07 kcal mol^{-1}.

3.4. Comparison of Interaction Energies. Although estimates of the interaction energies at the CCSD(T) CBS limit have been generated for each DFT optimized structure, the DFT interaction energies are also of interest. For the stationary points that we were able to locate, Table 2 lists the deviations of the MP2, B97-D, ωB97X-D, and M06-2X interaction energies computed with the haTZ basis set from the average of the CCSD(T) CBS limits in last 3 columns of Table 1). The results are entirely consistent with previous efforts to calibrate these methods against CCSD(T) CBS limit interaction energies.[66−68] Therefore, we will only briefly summarize the results here.

Statistically, the MP2, B97-D, ωB97X-D, and M06-2X methods exhibit very similar performance with average absolute deviations of 0.24, 0.35, 0.26, and 0.29 kcal mol^{-1}, respectively, whereas the corresponding deviation for the B3LYP interaction

Table 2. Deviations of MP2/haTZ and DFT/haTZ Interaction Energes (ΔE_{int} in kcal mol^{-1}) from the Average of the CCSD(T)/CBS Interaction Energies (E_{int}^{avg} in kcal mol^{-1})

structure	CCSD(T)/CBS E_{int}^{avg}	MP2 ΔE_{int}	B3LYP ΔE_{int}	B97-D ΔE_{int}	ωB97X-D ΔE_{int}	M06-2X ΔE_{int}
CH$_4$/H$_2$O						
OH···C	−0.99 ± 0.02	−0.00	+0.68	−0.35	−0.04	−0.08
CH···O	−0.65 ± 0.01	−0.01	+0.42	+0.11	+0.17	+0.16
C$_2$H$_6$/H$_2$O						
CH···O	−1.34 ± 0.02	−0.02	a	−0.37	+0.02	−0.14
OH···C	−1.10 ± 0.02	−0.07	+0.74	−0.40	−0.04	−0.07
C$_2$H$_2$/H$_2$O						
CH···O	−2.87 ± 0.02	−0.09	+0.47	+0.34	+0.11	+0.04
CH···O(p)	−2.87 ± 0.01	−0.09	+0.48	+0.40	+0.16	+0.04
OH···π	−2.55 ± 0.07	−0.27	+0.64	−0.30	−0.16	−0.26
OH$_2$···π	−1.93 ± 0.05	−0.10	+0.77	−0.23	−0.31	−0.44
C$_4$H$_2$/H$_2$O						
CH···O	−3.38 ± 0.02	−0.12	+0.55	+0.49	+0.16	+0.05
CH···O(p)	−3.38 ± 0.02	−0.12	+0.55	+0.53	+0.20	+0.05
OH···π	−2.28 ± 0.07	−0.30	+0.82	−0.23	−0.06	a
OH$_2$···π	−1.81 ± 0.05	−0.17	a	−0.19	−0.28	a
C$_2$H$_4$/H$_2$O						
OH···π	−2.53 ± 0.03	−0.33	+0.72	−0.47	−0.27	−0.30
CH$_2$···O	−0.84 ± 0.02	−0.09	+0.54	+0.16	+0.19	+0.07
CH$_2$···O(π)	−1.32 ± 0.03	−0.08	+0.80	+0.27	+0.25	+0.04
C$_4$H$_6$/H$_2$O						
CH···O	−1.15 ± 0.01	−0.06	+0.54	+0.17	+0.21	+0.21
CH$_2$···O	−1.52 ± 0.02	−0.14	+0.86	+0.28	+0.25	+0.07
OH···π	−2.97 ± 0.04	−0.47	+1.18	−0.53	−0.53	−0.68
C$_4$H$_4$/H$_2$O						
CH···O(p)	−1.40 ± 0.01	−0.11	+0.54	+0.20	+0.20	+0.19
CH···O	−1.52 ± 0.02	−0.14	+0.53	+0.17	+0.12	+0.17
OH···π	−2.74 ± 0.05	−0.72	+0.88	−0.64	−0.38	a
OH$_2$···π	−3.23 ± 0.05	−0.70	+1.06	−0.93	−0.65	−0.92
C$_5$H$_6$/H$_2$O						
CH···O	−1.30 ± 0.02	−0.12	+0.60	+0.20	+0.18	+0.27
OH···π	−3.79 ± 0.05	−0.67	+1.63	a	a	a
OH$_2$···π	−3.77 ± 0.05	−0.58	+1.91	−0.70	−0.70	−1.06
C$_6$H$_6$/H$_2$O						
CH···O	−1.28 ± 0.02	−0.11	+0.62	a	a	+0.27
CH···O(np)	−1.48 ± 0.02	−0.14	+0.63	+0.23	+0.23	+0.27
CH···O(p)	−1.28 ± 0.02	−0.11	+0.62	+0.20	+0.23	+0.27
OH···π	−3.21 ± 0.05	−0.63	+1.68	−0.32	−0.49	−0.71
OH$_2$···π	−3.14 ± 0.04	−0.57	+1.89	−0.34	−0.58	−0.77
max. absolute deviation		0.72	1.91	0.93	0.70	1.06
min. absolute deviation		0.00	0.42	0.11	0.02	0.04
avg. absolute deviation		0.24	0.83	0.35	0.26	0.29

^{a}Collapses to different stationary point. (See text for details.)

energies is significantly larger (0.83 kcal mol^{-1}). The data in Table 2 indicate that the OH···π and OH$_2$···π configurations of water interacting with the face of cyclic hydrocarbons (cyclobutadiene, cyclopentadiene, and benzene) are particularly challenging. This class of structures produces the maximum absolute deviation for each method (0.72, 1.91, 0.93, 0.70 and 1.06 kcal mol^{-1} for MP2, B3LYP, B97-D, ωB97X-D, and M06-2X, respectively).

The interaction energies corresponding to the deviations reported in Table 2 are provided in Table 5 for the stationary points that were located. In this format, some additional trends are more apparent. The B3LYP density functional yields significantly smaller interaction energies for hydrocarbon/water structures than the MP2 method but still maintains the same

energetic ordering (i.e., smallest to largest E$_{int}$ for a particular dimer). The B97-D functional produces interaction energies that more closely match the MP2 values (particularly for OH···π type structures and the ethane/water structures), but it does not maintain the energetic ordering in some cases (e.g., in the acetylene/water complexes and the cyclobutadiene/ water complexes). The ωB97X-D and M06-2X functionals match the MP2 energetic ordering of the hydrocarbon/ water interactions, and, despite some variation, their E$_{int}$ values closely resemble the energetics of those at the MP2 level of theory.

3.5. Comparison of Hessian Indices. The number of imaginary vibrational frequencies, n$_i$, associated with each MP2 and DFT optimized structure is also presented in Table 5.

Table 3. Intermolecular Distance (R in Å) for the MP2 Optimized Structures and the Deviations (ΔR and RMSD in Å) of the DFT Optimized Strutures from the MP2 Reference Geometries.

	MP2	B3LYP		B97-D		ωB97X-D		M06-2X	
structure	R	ΔR	rmsd	ΔR	rmsd	ΔR	rmsd	ΔR	rmsd
CH_4/H_2O									
OH···C	2.54	+0.19	0.10	+0.01	0.10	+0.00	0.06	−0.11	0.05
CH···O	2.64	+0.17	0.08	+0.11	0.06	+0.08	0.04	+0.10	0.05
C_2H_6/H_2O									
CH···O	2.74	a	a	+0.18	0.09	+0.18	0.07	−0.09	0.05
OH···C	2.52	+0.23	0.18	+0.04	0.21	+0.02	0.06	−0.09	0.04
C_2H_2/H_2O									
CH···O	2.20	+0.03	0.02	+0.15	0.11	−0.01	0.11	−0.01	0.02
CH···O(p)	2.19	+0.04	0.01	+0.17	0.08	−0.01	0.02	−0.00	0.01
OH···π	2.35	+0.10	0.05	+0.12	0.06	+0.04	0.04	+0.00	0.03
OH_2···π	2.95	+0.17	0.09	−0.06	0.03	−0.01	0.01	−0.10	0.05
C_4H_2/H_2O									
CH···O	2.15	+0.04	0.03	+0.16	0.14	+0.00	0.13	−0.00	0.02
CH···O(p)	2.15	+0.03	0.01	+0.17	0.08	+0.00	0.02	−0.00	0.02
OH···π	2.40	+0.18	0.22	+0.11	0.07	+0.07	0.12	a	a
OH_2···π	3.41	a	a	−0.05	0.06	+0.04	0.36	a	a
C_2H_4/H_2O									
OH···π	2.37	+0.12	0.08	+0.08	0.04	+0.03	0.03	+0.01	0.20
CH_2···O	2.96	+0.27	0.13	+0.20	0.10	+0.10	0.05	−0.01	0.01
CH···O(π)	2.73	+0.21	0.10	+0.15	0.08	+0.06	0.03	−0.07	0.04
C_4H_6/H_2O									
CH···O	2.48	+0.13	0.11	+0.12	0.06	+0.05	0.02	+0.03	0.01
CH_2···O	2.65	+0.24	0.10	+0.04	0.12	+0.08	0.03	−0.03	0.03
OH···π	2.47	+0.04	0.47	+0.19	0.16	+0.25	0.15	+0.10	0.12
C_4H_4/H_2O									
CH···O(p)	2.42	+0.11	0.04	+0.13	0.06	+0.03	0.03	+0.02	0.02
CH···O	2.40	+0.10	0.05	+0.13	0.14	+0.04	0.21	+0.03	0.06
OH···π	2.30	+0.15	0.28	+0.10	0.14	+0.06	0.14	a	a
OH_2···π	2.32	+0.11	0.44	+0.23	0.19	+0.25	0.15	+0.24	0.19
C_5H_6/H_2O									
CH···O	2.45	+0.13	0.13	+0.12	0.24	+0.04	0.25	+0.04	0.02
OH···π	2.35	+0.11	0.31	a	a	a	a	a	a
OH_2···π	2.61	+0.24	0.11	−0.03	0.02	+0.05	0.02	−0.02	0.03
C_6H_6/H_2O									
CH···O	2.46	+0.15	0.06	a	a	a	a	+0.05	0.02
CH···O(np)	2.42	+0.14	0.05	+0.14	0.06	+0.05	0.02	+0.04	0.01
CH···O(p)	2.46	+0.15	0.06	+0.13	0.06	+0.06	0.02	+0.04	0.01
OH···π	2.51	+0.09	0.36	+0.05	0.02	+0.13	0.11	+0.09	0.13
OH_2···π	2.75	+0.34	0.14	−0.03	0.01	+0.03	0.02	−0.06	0.02
max. absolute deviation		0.34	0.47	0.23	0.24	0.25	0.36	0.24	0.20
min. absolute deviation		0.03	0.01	0.01	0.01	0.00	0.01	0.00	0.01
avg. absolute deviation		0.14	0.14	0.11	0.09	0.06	0.08	0.05	0.05

^{a}Collapses to different stationary point. (See text for details.)

Recall that we were not able to locate two stationary points with the B3LYP, B97-D, and ωB97X-D functionals, while four could not be located with M06-2X. Of the 28 structures optimized with B3LYP and B97-D, nine had a different Hessian index (or number of imaginary frequencies) than obtained from MP2 calculations. The number of discrepancies increases to eleven for ωB97X-D. For the 26 stationary points optimized with the M06-2X density functional, n_i differed in nine cases. The magnitudes of the offending frequencies (real or imaginary) were generally rather sizable, making it unlikely that the discrepancies could be attributed to numerical issues, especially given the tight convergence criteria and dense numerical integration grids employed in this work. Only in the

case of one discrepancy were the magnitudes of both the MP2 reference frequency and the DFT frequency less than 10 cm^{-1}. All vibrational frequencies are reported in the Supporting Information so that interested readers can directly compare the MP2 and DFT vibrational frequencies.

Our research group has previously observed a similar phenomenon when we noted that many popular density functionals had problems reproducing CCSD(T) Hessian indices for some rather challenging saddle points on the water dimer PES.[105] For $(H_2O)_2$, discrepancies were encountered for second- and third-order saddle points. In the present situation, however, there is often disagreement over whether or not a particular structure is a minimum on the PES.

Table 4. CCSD(T) CBS Limit Interaction Energy^a ($E_{int}^{CCSD(T)/CBS}$ in kcal mol^{-1}) Obtained with MP2 Optimized Structures and Deviations ($\Delta E_{int}^{CCSD(T)/CBS}$ in kcal mol^{-1}) When Using DFT Optimized Structures

structure	$E_{int}^{CCSD(T)/CBS}$	$E_{int}^{CCSD(T)/CBS}$			
	MP2	B3LYP	B97-D	ωB97X-D	M06-2X
CH$_4$/H$_2$O					
OH···C	−0.99	+0.07	+0.02	+0.01	+0.04
CH···O	−0.66	+0.04	+0.01	+0.01	+0.02
C$_2$H$_6$/H$_2$O					
CH···O	−1.35	b	+0.03	+0.03	+0.06
OH···C	−1.11	+0.09	+0.04	+0.01	+0.04
C$_2$H$_2$/H$_2$O					
CH···O	−2.88	+0.00	+0.12	+0.04	+0.00
CH···O(p)	−2.89	+0.00	+0.08	+0.01	+0.00
OH···π	−2.51	−0.01	+0.00	−0.02	−0.01
OH$_2$···π	−1.93	+0.06	+0.02	−0.01	+0.05
C$_4$H$_2$/H$_2$O					
CH···O	−3.40	+0.00	+0.14	+0.04	−0.00
CH···O(p)	−3.40	+0.00	+0.13	+0.01	+0.00
OH···π	−2.24	−0.00	+0.00	−0.02	b
OH$_2$···π	−1.81	b	+0.02	−0.06	b
C$_2$H$_4$/H$_2$O					
OH···π	−2.54	+0.02	−0.01	−0.01	+0.03
CH$_2$···O	−0.86	+0.10	+0.06	+0.02	−0.00
CH$_2$···O(π)	−1.35	+0.13	+0.07	+0.03	+0.03
C$_4$H$_6$/H$_2$O					
CH···O	−1.16	+0.03	+0.02	+0.01	−0.00
CH$_2$···O	−1.53	+0.11	+0.07	+0.01	+0.01
OH···π	−2.99	+0.27	−0.02	−0.04	+0.04
C$_4$H$_4$/H$_2$O					
CH···O(p)	−1.41	+0.09	−0.03	−0.03	−0.00
CH···O	−1.53	+0.27	+0.01	−0.05	−0.00
OH···π	−2.75	+0.02	+0.03	−0.00	b
OH$_2$···π	−3.25	+0.01	+0.04	+0.03	−0.00
C$_5$H$_6$/H$_2$O					
CH···O	−1.31	+0.03	+0.04	+0.05	+0.00
OH···π	−3.81	+0.41	b	b	b
OH$_2$···π	−3.80	+0.22	+0.01	−0.03	+0.03
C$_6$H$_6$/H$_2$O					
CH···O	−1.30	+0.04	b	b	−0.02
CH···O(np)	−1.50	+0.03	+0.03	−0.02	−0.02
CH···O(p)	−1.31	+0.03	+0.02	−0.02	−0.02
OH···π	−3.24	+0.39	−0.04	−0.01	+0.07
OH$_2$···π	−3.18	+0.29	+0.01	−0.04	+0.03
max. absolute deviation		0.41	0.14	0.06	0.07
min. absolute deviation		0.00	0.00	0.00	0.00
avg. absolute deviation		0.10	0.04	0.02	0.02

^{a}$E_{int}^{CCSD(T)/CBS} = E_{int}^{MP2/CBS} + \delta_{MP2}^{CCSD(T)}$. ^{b}Collapses to different stationary point. (See text for details.)

4. CONCLUSION

To investigate the structures, energetics, and nature of hydrocarbon/water interactions, 30 hydrocarbon/water dimer configurations were examined. Full geometry optimizations were performed at the MP2 level of theory, as well with the B3LYP, B97-D, ωB97X-D, and M06-2X density functional methods. The corresponding vibrational frequencies were also computed for each stationary point identified. Explicitly correlated MP2-R12 computations were combined with a higher order correlation correction to estimate CCSD(T) CBS limit interaction energies. For MP2 optimized structures, CCSD(T) CBS limit interaction energies were also estimated using the CCSD(T)-F12 method both with and without CP

corrections for BSSE. The three estimates of E_{int} at the CCSD(T) CBS limit consistently gave very similar values, never deviating by more than ±0.07 kcal mol^{-1} from their mean. In some cases these interaction energies were quite substantial (as large as −3.79 ± 0.05 kcal mol^{-1} for the OH···π structure of the cyclobutadiene/water dimer).

For OH···π structures, MP2 tends to slightly overestimate the magnitude of E_{int} relative to CCSD(T) values obtained with the haTZ basis set. The differences can exceed 0.3 kcal mol^{-1} (or roughly 10%) and grow as large as 0.40 kcal mol^{-1} for the cyclobutadiene/water dimer. In contrast, the MP2 and CCSD(T) interaction energies never deviated by more than 0.04 kcal mol^{-1} for the CH···O structures.

Table 5. Number of Imaginary Vibrational Frequencies (n_i) and Interaction Energes (E_{int} in kcal mol^{-1}) for MP2 and DFT Optimized Hydrocarbon/Water Structures

structure	MP2		B3LYP		B97-D		ωB97X-D		M06-2X	
	n_i	E_{int}	n_i	E_{int}	n_i	E_{int}	n_i	E_{int}	n_i	E_{int}
CH_4/H_2O										
OH···C	0	−0.99	0	−0.31	0	−1.34	1	−1.03	0	−1.07
CH···O	0	−0.66	1	−0.24	2	−0.55	0	−0.49	0	−0.49
C_2H_6/H_2O										
CH···O	0	−1.36		a	0	−1.71	0	−1.32	0	−1.49
OH···C	0	−1.17	0	−0.36	0	−1.50	0	−1.15	0	−1.18
C_2H_2/H_2O										
CH···O	0	−2.97	0	−2.40	0	−2.53	0	−2.77	0	−2.84
CH···O(p)	1	−2.96	1	−2.40	1	−2.47	1	−2.71	0	−2.83
OH···π	0	−2.82	0	−1.91	0	−2.84	0	−2.71	0	−2.80
OH$_2$···π	1	−2.03	1	−1.16	1	−2.16	1	−2.24	1	−2.37
C_4H_2/H_2O										
CH···O	0	−3.51	0	−2.83	0	−2.90	0	−3.22	0	−3.34
CH···O(p)	1	−3.51	1	−2.83	1	−2.85	1	−3.19	0	−3.34
OH···π	0	−2.58	0	−1.46	0	−2.51	0	−2.34		a
OH$_2$···π	1	−1.97		a	1	−1.99	2	−2.09		a
C_2H_4/H_2O										
OH···π	0	−2.86	0	−1.80	0	−2.99	0	−2.79	0	−2.82
CH$_2$···O	2	−0.93	2	−0.31	2	−0.68	0	−0.65	0	−0.77
CH$_2$···O(π)	1	−1.41	2	−0.52	1	−1.05	1	−1.07	1	−1.28
C_4H_6/H_2O										
CH···O	1	−1.21	2	−0.62	2	−0.98	2	−0.94	1	−0.95
CH$_2$···O	1	−1.66	2	−0.65	1	−1.23	1	−1.26	1	−1.45
OH···π	0	−3.44	2	−1.80	0	−3.50	1	−3.51	0	−3.65
C_4H_4/H_2O										
CH···O(p)	1	−1.50	2	−0.86	2	−1.20	2	−1.20	1	−1.21
CH···O	0	−1.65	0	−0.99	0	−1.35	1	−1.40	0	−1.35
OH···π	0	−3.46	0	−1.86	0	−3.38	0	−3.12		a
OH$_2$···π	0	−3.93	0	−2.17	0	−4.16	0	−3.87	0	−4.14
C_5H_6/H_2O										
CH···O	1	−1.42	0	−0.70	2	−1.09	1	−1.12	2	−1.03
OH···π	0	−4.46	0	−2.16		a		a		a
OH$_2$···π	1	−4.36	1	−1.86	0	−4.47	0	−4.48	0	−4.84
C_6H_6/H_2O										
CH···O	1	−1.39	1	−0.67		a		a	0	−1.01
CH···O(np)	1	−1.62	0	−0.84	2	−1.25	1	−1.25	0	−1.21
CH···O(p)	1	−1.40	1	−0.67	2	−1.08	2	−1.05	0	−1.01
OH···π	0	−3.85	1	−1.54	1	−3.54	1	−3.70	0	−3.92
OH$_2$···π	1	−3.71	1	−1.25	2	−3.48	0	−3.71	0	−3.91

^{a}Collapses to different stationary point. (See text for details.)

All four density functionals examined, including B3LYP, produced reasonable optimized structures for high-level single energy point energy calculations to estimate the CCSD(T) CBS limit interaction energies. Using B3LYP optimized structures instead of MP2 ones to determine E_{int} at the CCSD(T) CBS limit only introduces an absolute deviation of 0.10 kcal mol^{-1} on average, while the average absolute deviation introduced with B97-D, ωB97X-D, and M06-2X structures is 0.04 kcal mol^{-1} or less. Although B3LYP provided reasonable optimized geometries, it did not give reliable E_{int} values. The other functionals performed much better for E_{int}, similar to MP2 on average. The average absolute deviations from the CCSD(T) CBS limit interaction energies ranged from 0.24−0.35 kcal mol^{-1} for the MP2, B97-D, ωB97X-D, and M06-2X methods.

Of the 30 stationary points identified via MP2 optimizations, we were not able to located 2 stationary points on the B3LYP,

B97-D, and ωB97X-D PESs using common optimization procedures. With M06-2X, 4 structures were not located. These results are perhaps not unexpected given the flat nature of the PESs being explored. However, even when the same structure was optimized with the MP2 and DFT methods, the corresponding frequency calculations yielded different Hessian indices (or number of imaginary vibrational frequencies) in a third of the cases. For the 28 structures identified, the value of n_i from B3LYP, B97-D, and ωB97X-D frequency calculations differed from the MP2 Hessian index in 9, 9, and 11 cases, respectively. For the M06-2X functional, 9 of the 26 frequency calculations gave a Hessian index that differed from the MP2 values. One interpretation of these results is that the MP2 results are incorrect. Given the general agreement between MP2 and CCSD(T) results, this possibility seems unlikely, particularly in cases where there is no concensus among the DFT methods regarding the Hessian index. Instead, it seems

more plausible that these results should raise some concerns about the use of popular density functional methods to locate and characterize (i.e., minimum or *n*-th order saddle point) stationary points on the PESs of noncovalent complexes. The data also suggest that the development and validation of DFT methods for the reliable description of noncovalent interactions may require more than calibration against carefully curated benchmark databases of interaction energies.

■ ASSOCIATED CONTENT

Ⓢ Supporting Information

Cartesian coordinates of MP2 optimized hydrocarbon/water geometries. CCSD(T) CBS limit interaction energy calculations for DFT optimized structures. Vibrational frequencies. This material is available free of charge via the Internet at http://pubs.acs.org.

■ AUTHOR INFORMATION

Corresponding Author

*To whom correspondence should be addressed E-mail: tschumpr@olemiss.edu

Notes

The authors declare no competing financial interest.

■ ACKNOWLEDGMENTS

■ REFERENCES

(1) *Protein Structure*; Scheraga, H. A., Ed.; Academic Press: New York, 1961.

(2) *Molecular Interactions from van der Waals to Strongly Bound Complexes*, 3rd ed.; Scheiner, S., Ed.; John Wiley and Sons: Chichester, England, 1997.

(3) McGaughey, G. B.; Gagne, M.; Rappe, A. K. *J. Biol. Chem.* **1998**, *273*, 15458−15463.

(4) Šponer, J.; Jurecka, P.; Marchan, I.; Luque, F. J.; Orozco, M.; Hobza, P. *Chem. Eur. J.* **2006**, *12*, 2854−2865.

(5) Glasstone, S. *Trans. Faraday Soc.* **1937**, *33*, 200−206.

(6) Allerhand, A.; von Rague Schleyer, P. *J. Am. Chem. Soc.* **1963**, *85*, 1715−1723.

(7) *The Weak Hydrogen Bond in Structural Chemistry and Biology*; Desiraju, G. R., Steiner, T., Eds.;Oxford University Press: Oxford, 1999.

(8) Hobza, P.; Havlas, Z. *Chem. Rev.* **2000**, *100*, 4253−4264.

(9) Nishio, M. *CrystEngComm* **2004**, *6*, 130−158.

(10) Desiraju, G. R. *Chem. Commun.* **2005**, 2995−3001.

(11) Scheiner, S. In *Theory and Applications of Computational Chemistry; The First Forty Years*; Dykstra, C., Frenking, G., Kim, K., Scuseria, G., Eds.; Elsevier: Amsterdam, 2005; pp 831−857.

(12) Wulf, O. R.; Liddel, U.; Hendricks, S. B. *J. Am. Chem. Soc.* **1936**, *58*, 2287−2293.

(13) Levitt, M.; Perutz, M. F. *J. Mol. Biol.* **1988**, *201*, 751−754.

(14) Suzuki, S.; Green, P. G.; Bumgarner, R. E.; Dasgupta, S.; Goddard, W. A.; Blake, G. A. *Science* **1992**, *257*, 942−945.

(15) Peterson, K. I.; Klemperer, W. *J. Chem. Phys.* **1984**, *81*, 3842−3845.

(16) Peterson, K. I.; Klemperer, W. *J. Chem. Phys.* **1986**, *85*, 725−732.

(17) Rovira, M. C.; Novoa, J. J.; Whangbo, M.; Williams, J. M. *Chem. Phys.* **1995**, *200*, 319−335.

(18) Tsuzuki, S.; Honda, K.; Uchimaru, T.; Mikami, M.; Tanabe, K. *J. Am. Chem. Soc.* **2000**, *122*, 3746−3753.

(19) Tzeli, D.; Mavridis, A.; Xantheas, S. S. *J. Chem. Phys.* **2000**, *112*, 6178−6189.

(20) Scheiner, S.; Grabowski, S. J.; Kar, T. *J. Phys. Chem. A* **2001**, *105*, 10607−10612.

(21) Jing, Y.; Li, Z.; Wu, D.; Li, Y.; Wang, B.; Sun, C. *J. Phys. Chem. A* **2006**, *110*, 7470−7476.

(22) Ostojić, B. D.; Janjić, G. V.; Zarić, S. D. *Chem. Commun.* **2008**, 6546−6548.

(23) Li, Q.; An, X.; Luan, F.; Li, W.; Gong, B.; Cheng, J.; Sun, J. *Int. J. Quantum Chem.* **2008**, *108*, 558−566.

(24) Tsuzuki, S.; Fujii, A. *Phys. Chem. Chem. Phys.* **2008**, *10*, 2584−2594.

(25) Slipchenko, L. V.; Gordon, M. S. *J. Phys. Chem. A* **2009**, *113*, 2092−2102.

(26) Martins, J. B. L.; Politi, J. R. S.; Garcia, E.; Vilela, A. F. A.; Gargano, R. *J. Phys. Chem. A* **2009**, *113*, 14818−14823.

(27) Domagala, M.; Grabowski, S. J. *Chem. Phys.* **2010**, *367*, 1−6.

(28) Mackie, I. D.; DiLabio, G. A. *J. Phys. Chem. A* **2008**, *112*, 10968−10976.

(29) Woon, D. E.; Zeng, P.; Beck, D. R. *J. Chem. Phys.* **1990**, *93*, 7808−7812.

(30) Novoa, J. J.; Tarron, B.; Whangbo, M.; Williams, J. M. *J. Chem. Phys.* **1991**, *95*, 5179−5186.

(31) Szczesniak, M. M.; Chalasinski, G.; Cybulski, S. M.; Cieplak, P. *J. Chem. Phys.* **1993**, *98*, 3078−3089.

(32) Suenram, R. D.; Fraser, G. T.; Lovas, F. J.; Kawashima, Y. *J. Chem. Phys.* **1994**, *101*, 7230−7240.

(33) Dore, L.; Cohen, R. C.; Schmuttenmaer, C. A.; Busarow, K. L.; Elrod, M. J.; Loeser, J. G.; Saykally, R. J. *J. Chem. Phys.* **1994**, *100*, 863−876.

(34) Kryachko, E. S.; Zeegers-Huyskens, T. *J. Phys. Chem. A* **2001**, *105*, 7118−7125.

(35) Akin-Ojo, O.; Szalewicz, K. *J. Chem. Phys.* **2005**, *123*, 134311.

(36) Udagawa, T.; Ishimoto, T.; Tokiwa, H.; Tachikawa, M.; Nagashima, U. *J. Phys. Chem. A* **2006**, *110*, 7279−7285.

(37) Raghavendra, B.; Arunan, E. *Chem. Phys. Lett.* **2008**, *467*, 37−40.

(38) Hartmann, M.; Wetmore, S. D.; Radom, L. *J. Phys. Chem. A* **2001**, *105*, 4470−4479.

(39) Engdahl, A.; Nelander, B. *Chem. Phys. Lett.* **1983**, *100*, 129−132.

(40) Frisch, M. J.; Pople, J. A.; Del Bene, J. E. *J. Chem. Phys.* **1983**, *78*, 4063−4065.

(41) Block, P. A.; Marshall, M. D.; Pedersen, L. G.; Miller, R. E. *J. Chem. Phys.* **1992**, *96*, 7321−7332.

(42) Tzeli, D.; Mavridis, A.; Xantheas, S. S. *Chem. Phys. Lett.* **2001**, *340*, 538−546.

(43) Tzeli, D.; Mavridis, A.; Xantheas, S. S. *J. Phys. Chem. A* **2002**, *106*, 11327−11337.

(44) Chandra, A.; Pal, S. *Chem. Phys. Lett.* **1995**, *241*, 399−403.

(45) Engdahl, A.; Nelander, B. *J. Phys. Chem.* **1985**, *89*, 2860−2864.

(46) Wanna, J.; Menapace, J. A.; Bernstein, E. R. *J. Chem. Phys.* **1986**, *85*, 1795−1805.

(47) Engdahl, A.; Nelander, B. *J. Phys. Chem.* **1987**, *91*, 2253−2258.

(48) Gotch, A. J.; Zwier, T. S. *J. Chem. Phys.* **1992**, *96*, 3388−3401.

(49) Gutowsky, H. S.; Emilsson, T.; Arunan, E. *J. Chem. Phys.* **1993**, *99*, 4883−4893.

(50) Pribble, R. N.; Zwier, T. S. *Science* **1994**, *265*, 75−79.

(51) Pribble, R. N.; Garrett, A. W.; Haber, K.; Zwier, T. S. *J. Chem. Phys.* **1995**, *103*, 531−544.

(52) Cheng, B.-M.; Grover, J.; Walters, E. *Chem. Phys. Lett.* **1995**, *232*, 364−369.

(53) Fredericks, S. Y.; Jordan, K. D.; Zwier, T. S. *J. Phys. Chem.* **1996**, *100*, 7810−7821.

(54) Kim, K. S.; Lee, J. Y.; Choi, H. S.; Kim, J.; Jang, J. H. *Chem. Phys. Lett.* **1997**, *265*, 497−502.

(55) Zhao, Y.; Tishchenko, O.; Truhlar, D. G. *J. Phys. Chem. B* **2005**, *109*, 19046−19051.

(56) Min, S. K.; Lee, E. C.; Lee, H. M.; Kim, D. Y.; Kim, D.; Kim, K. S. *J. Comput. Chem.* **2008**, *29*, 1208−1221.

1655

dx.doi.org/10.1021/ct300132e | *J. Chem. Theory Comput.* 2012, 8, 1646−1656

(57) Li, S.; Cooper, V. R.; Thonhauser, T.; Puzder, A.; Langreth, D. C. *J. Phys. Chem. A* **2008**, *112*, 9031−9036.

(58) Prakash, M.; Samy, K. G.; Subramanian, V. *J. Phys. Chem. A* **2009**, *113*, 13845−13852.

(59) Ma, J.; Alfe, D.; Michaelides, A.; Wang, E. *J. Chem. Phys.* **2009**, *130*, 154303.

(60) Kim, S.-J.; Seo, H.-I.; Boo, B. H. *Mol. Phys.* **2009**, *107*, 1261−1270.

(61) Ran, J.; Hobza, P. *J. Chem. Theory Comput.* **2009**, *5*, 1180−1185.

(62) Gierszal, K. P.; Davis, J. G.; Hands, M. D.; Wilcox, D. S.; Slipchenko, L. V.; Ben-Amotz, D. *J. Phys. Chem. Lett.* **2011**, *2*, 2930−2933.

(63) Gu, Y.; Kar, T.; Scheiner, S. *J. Am. Chem. Soc.* **1999**, *121*, 9411−9422.

(64) Alabugin, I. V.; Manoharan, M.; Peabody, S.; Weinhold, F. *J. Am. Chem. Soc.* **2003**, *125*, 5973−5987.

(65) Mackie, I. D.; DiLabio, G. A. *J. Phys. Chem. A* **2008**, *112*, 10968−10976.

(66) Vázquez-Mayagoitia, A.; Sherrill, C. D.; Aprá, E.; Sumpter, B. G. *J. Chem. Phys.* **2010**, *6*, 727−734.

(67) Thanthiriwatte, K. S.; Hohenstein, E. G.; Burns, L. A.; Sherrill, C. D. *J. Chem. Theory Comput.* **2011**, *7*, 88−96.

(68) Burns, L.; Vázquez-Mayagoitia, A.; Sumpter, B. G.; Sherrill, C. D. *J. Chem. Phys.* **2011**, *134*, 084107.

(69) Becke, A. D. *J. Chem. Phys.* **1993**, *98*, 5648.

(70) Lee, C.; Yang, W.; Parr, R. G. *Phys. Rev. B.* **1988**, *37*, 785−789.

(71) Grimme, S. *J. Comput. Chem.* **2006**, *27*, 1787−1799.

(72) Chai, J.; Head-Gordon, M. *Phys. Chem. Chem. Phys.* **2008**, *10*, 6615−6620.

(73) Zhao, Y.; Truhlar, D. G. *Theor. Chim. Acta* **2008**, *120*, 215−241.

(74) Kutzelnigg, W. *Theor. Chim. Acta* **1985**, *68*, 445−469.

(75) Klopper, W.; Kutzelnigg, W. *Chem. Phys. Lett.* **1987**, *134*, 17−22.

(76) Kutzelnigg, W.; Klopper, W. *J. Chem. Phys.* **1991**, *94*, 1985−2001.

(77) Klopper, W.; Manby, F. R.; Ten-No, S.; Valeev, E. F. *Int. Rev. Phys. Chem.* **2006**, *25*, 427−468.

(78) Klopper, W.; Kutzelinigg, W.; Müller, H.; Noga, J.; Vogtner, S. *Top. Curr. Chem.* **1999**, *203*, 21−41.

(79) Klopper, W. *J. Chem. Phys.* **1995**, *102*, 6168−6179.

(80) Valeev, E. F. *Chem. Phys. Lett.* **2004**, *395*, 190−195.

(81) Valeev, E. F.; Allen, W. D.; Hernandez, R.; Sherrill, C. D.; Schaefer, H. F. III *J. Chem. Phys.* **2003**, *118*, 8594−8610.

(82) Jurečka, P.; Šponer, J.; Černý, J.; Hobza, P. *Phys. Chem. Chem. Phys.* **2006**, *8*, 1985−1993.

(83) Sinnokrot, M.; Sherrill, C. *J. Phys. Chem. A* **2006**, *110*, 10656−10668.

(84) Tsuzuki, S.; Uchimaru, T. *Curr. Org. Chem.* **2006**, *10*, 745−762.

(85) Hobza, P.; Zahradnik, R.; Müller-Dethlefs, K. *Collect. Czech. Chem. Commun.* **2006**, *71*, 443−531.

(86) Tschumper, G. S. In *Reviews in Computational Chemistry*; Lipkowitz, K. B., Cundari, T. R., Eds.; Wiley-VCH, Inc.: Hoboken, NJ, 2009; Vol. *26*, Chapter 2, pp 39−90.

(87) Knizia, G.; Adler, T. B.; Werner, H. *J. Chem. Phys.* 2009, *054104*, 130.

(88) Adler, T. B.; Knizia, G.; Werner, H. *J. Chem. Phys.* **2007**, *127*, 221106.

(89) Peterson, K. A.; Adler, T. B.; Werner, H. *J. Chem. Phys.* **2008**, *128*, 084102.

(90) Werner, H.-J. et al. MOLPRO, version 2009.1, a package of ab initio programs. 2009. See http://www.molpro.net (accessed April 3, 2012).

(91) Frisch, M. J. et al. Gaussian 03, Revision E.01. Gaussian, Inc.: Wallingford, CT, 2004.

(92) Frisch, M. J. et al. Gaussian 09, Revision A.1. Gaussian, Inc.: Wallingford CT, 2009.

(93) Janssen, C. L.; Nielsen, I. B.; Leininger, M. L.; Valeev, E. F.; Seidl, E. T. The Massively Parallel Quantum Chemistry Program (MPQC) Version 2.3.1. Sandia National Laboratories: Livermore, CA, USA, 2004. http://www.mpqc.org (accessed April 3, 2012).

(94) Valeev, E. F.; Janssen, C. L. *J. Chem. Phys.* **2004**, *121*, 1214−1227.

(95) Werner, H.-J. et al. MOLPRO, version 2006.1, a package of ab initio programs. 2006. http://www.molpro.net (accessed April 3, 2012).

(96) Kestner, N. R. *J. Chem. Phys.* **1968**, *48*, 252−257.

(97) Liu, B.; McLean, A. D. *J. Chem. Phys.* **1973**, *59*, 4557−4558.

(98) Jansen, H. B.; Ros, P. *Chem. Phys. Lett.* **1969**, *3*, 140−143.

(99) Boys, S. F.; Bernardi, F. *Mol. Phys.* **1970**, *19*, 553−566.

(100) Kestner, N. R.; Combariza, J. E. In *Reviews in Computational Chemistry*; Lipkowitz, K. B., Boyd, D. B., Eds.; Wiley-VCH Publishers: New York, 1999; Vol. *13*; Chapter 2, pp 99−132.

(101) Sherrill, C. D. In *Reviews in Computational Chemistry*; Lipkowitz, K. B., Cundari, T. R., Eds.; Wiley-VCH, Inc.: Hoboken, NJ, 2009; Vol. *26*; Chapter 1, pp 1−38.

(102) Lane, J. R.; Kjaergaard, H. G. *J. Chem. Phys.* **2009**, *131*, 034307.

(103) Tschumper, G. S.; Leininger, M. L.; Hoffman, B. C.; Valeev, E. F.; Schaefer, H. F. III; Quack, M. *J. Chem. Phys.* **2002**, *116*, 690−701.

(104) Ponder, J. W. TINKER - Software tools for molecular design, Version 5.1.09. Washington University School of Medicine: Saint Louis, MO, 2009.

(105) Anderson, J. A.; Tschumper, G. S. *J. Phys. Chem. A* **2006**, *110*, 7268−7271.